· Article ·
Advances in Polar Science
doi: 10.13679/j.advps.2014.1.00017
March 2014 Vol. 25 No. 1: 17-25

Petrography and mineralogy of new lunar meteorite MIL090036

XIE Lanfang[1,2], CHEN Hongyi[1,2], MIAO Bingkui[1,2*], XIA Zhipeng[1,2] & YAO Jie[1,2]

[1] Guangxi Scientific Experiment Center of Mining, Metallurgy and Environment, Guilin University of Technology, Guilin 541004, China;
[2] Guangxi Key Laboratory of Hidden Metallic Ore Deposits Exploration, Guilin 541004, China

Received 15 December 2013; accepted 4 March 2014

Abstract MIL090036 is a previously unknown meteorite (a feldspathic lunar breccia) that was discovered in Antarctica. The detailed petrography and mineralogy of this meteorite forms the subject of this paper. It has a typical clastic texture that consists of various types of rock debris (e.g. anorthosite, gabbroic anorthosite, gabbro, regolith breccia, troctolite, microporphyritic crystalline impact melt and compound clasts), mineral crystal fragments (e.g. pyroxenes, plagioclase, olivine and ilmenite) and feldspathic glass clasts. The fine-grained recrystallized minerals and mineral clasts are cemented together in a glassy groundmass. The anorthite content of plagioclase in the gabbro (An_{81-83}) and anorthosite (An_{88-93}) both have relatively low calcium content compared to those from other breccias (An_{90-98}). The pyroxene composition (Fs_{12-35} Wo_{3-44} En_{22-79}) in the rock debris, crystal mineral clasts and anorthositic glass clasts are relatively iron-deficient compared to those from gabbro debris with melt glass (Fs_{37-65} Wo_{10-29} En_{21-49}) and groundmass (Fs_{18-69} Wo_{3-45} En_{14-50}). In contrast, the pyroxene grains in the gabbroic anorthosite display a narrow compositional range (Fs_{24-27} Wo_{7-14} En_{59-69}). Olivine grains in mineral fragments and the groundmass have a wider compositional range (Fo_{57-79}) than those in the rock debris (Fo_{67-77}). The Fe/Mn ratio in olivine is in the range of 47 to 83 (average 76) and 76 to 112 (average 73) in pyroxenes, and hence classify within the lunar field. The characteristics of texture, mineral assemblage and compositions suggest that MIL090036 possibly originated from a region beyond that of the Apollo and Luna samples. Further study of MIL090036 is therefore likely to lead to a better understanding of the geological processes on the Moon and the chemical composition of the lunar crust.

Keywords **Lunar meteorite, MIL090036, Lunar breccias, Petrography, Mineralogy**

Citation: Xie L F, Chen H Y, Miao B K, et al. Petrography and Mineralogy of New Lunar Meteorite MIL090036. Adv Polar Sci, 2014, 25: 17-25, doi: 10.13679/j.advps.2014.1.00017

1 Introduction

There are currently three main ways to gather compositional information of the lunar crust: Remote sensing, lunar sampling and collection of lunar meteorites[1-2]. While remote sensing provides a "bird's eye view" of the EPMAUser Moon, the precision of the data is limited and cannot be used to research microscopic characteristics of the lunar crust, such as microstructure and micromorphology. Apollo and Luna sampling programs collected abundant lunar samples from different sites on the surface of the Moon over an area of only 5.4%–8.8% of the total surface[3]. Such *in-situ* sampling is costly and has not yet retrieved specimens from the far side of the Moon.

An important source of material that is representative of the lunar crust is lunar meteorites that were ejected from the surface of the Moon and captured by the gravitational field of the Earth. Compared with remote sensing and direct sampling, the collection and sampling of lunar meteorites found on Earth provide us a cost-effective way to study lunar material, which is likely more representative of the composition of the Moon's crust[3-4].

MIL090036 is a newly discovered lunar meteorite

* Corresponding author (email: miaobk@glut.edu.cn)

that was found in the Antarctic Miller Range Ice Field by the 2009–2010 ANSMET Program (Antarctic Search for Meteorites). Based on previous studies that included optical microscopy, resonance neutron activation analysis, electron microprobe analysis and cosmogenic nuclide studies, MIL090036 is a clast-rich, feldspathic breccia with a glassy-groundmass, and is mineralogically and petrologically similar to samples from the Apollo 16 sampling site[5-6]. Cosmogenic nuclide studies show that the meteorite has a 0.1–0.2 Ma terrestrial age[7]. We present a detailed petrographic and mineralogical study of MIL090036 which aims to better understand the composition of the Moon's crust.

2 Sample and analytical methods

MIL090036 which weighs 245 g, has a smooth surface with no fusion crust evident. Its interior structure is clearly brecciated with gray clasts dispersed in a dark groundmass[8]. The studied 30-μm-thick thin-section (MIL090036, 26) was provided by NASA (Figure 1) and was petrographically assessed using optical microscopy. Mineral compositions were analyzed using a JEOL JXA-8230 electron microprobe at the Guangxi Key Laboratory of Hidden Metallic Ore Deposits Exploration in the Guilin University of Technology. The accelerating voltages during the analysis of metal, silicate and oxide minerals were 20 kV, 15 kV and 15 kV, respectively. The beam current was 20 nA with a beam spot size of 5 μm, except for analysis of some very small mineral grains analyzed with a beam spot size of 1 μm. Bulk elemental composition was subsequently quantified using a 200 μm defocused electron beam, with data then normalized to 100%. Calibration of the samples was done against standards: silicates and metal minerals were calibrated against natural silicate and metal minerals respectively, and troilite was calibrated against oxide and sulfide. The measuring time of all the element-characteristic peaks and backgrounds were 10 s and 5 s, respectively with all raw analytical data corrected by the traditional ZAF method.

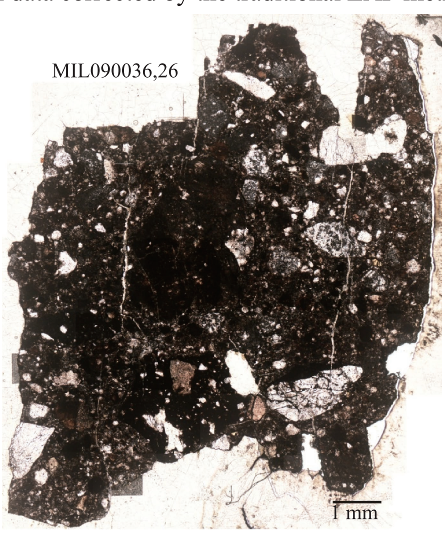

Figure 1 Transmitted-light photomicrograph of thin-section MIL090036, 26.

3 Petrography

MIL090036, 26 has a feldspathic lunar breccia texture (Figures 1–2) mainly composed of various types of lithic clasts (anorthosite, gabbroic anorthosite, gabbro, regolith breccia, troctolite, microporphyritic crystalline impact melt and compound clasts, Figure 3), mineral clasts (pyroxenes, plagioclase, olivine, with minor ilmenite) and glass clasts which are mainly plagioclase. The matrix is composed of fine-grained plagioclase, pyroxenes, and minor olivine, ilmenite and glass. The content of plagioclase and pyroxene in the matrix reaches 60 vol.%.

Figure 2 Backscattered electron (BSE) image of thin-section MIL090036, 26. Clasts discussed in the text are shown in white squares: Anorthosite clasts (**a**); Gabbroic anorthosite clasts (**b**); Troctolite clasts (**c**); Homeocrystalline gabbor clasts (**d**); Gabbro clasts with glass (**e**); Polymict clasts (**f**); Microporphyritic crystalline impact melt breccia (**g**); Glass melt breccia (**h**–**i**); Regolith clasts (**j**); Kamacite graint (**k**); Pyroxene crystalloclastic (**l**).

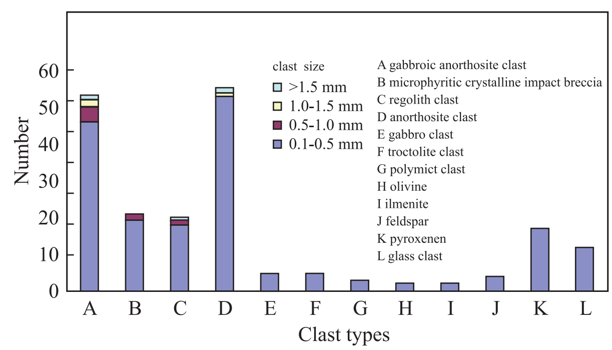

Figure 3 Frequency distribution of breccias in MIL090036, 26, which are greater than 0.1 mm in size.

The main breccias of MIL090036, 26 are composed of anorthosite clasts and gabbroic anorthosite clasts (0.1–0.5 mm in size). The lithic clasts are mainly composed of plagioclase and pyroxene, with olivine as the main constituent of the troctolite clasts. Plagioclases in both mineral and lithic clasts have the same characteristics-clear mineral boundaries and a strongly broken texture. Plagioclase in the glassy clasts has no observed broken characteristic (Figure 4). The pyroxenes vary texturally between clasts: pyroxene in lithic and glass clasts are euhedral-subeuhedral-anhedral, while in mineral clasts they are subeuhedral-euhedral, and most show exsolution textures (Figure 4i). Ilmenite was discovered in nearly all types of clasts, as well as minor amounts of troilite and ferronickel. Ilmenite, troilite and ferronickel are randomly distributed with a "star-like" appearance in the various clasts. Further characteristics of the clasts are summarized in Table 1.

The matrix of MIL090036, 26 is glassy and contains fine-grained recrystallized plagioclase, pyroxene, olivine, ilmenite, quartz and other opaque minerals (<30 μm in size), these minerals comprise approximately 60 vol.% of the matrix and have similar characteristics within mineral clasts, except for being of a smaller size.

4 Mineral chemistry

4.1 Plagioclase

The plagioclases in MIL090036, 26 are predominantly

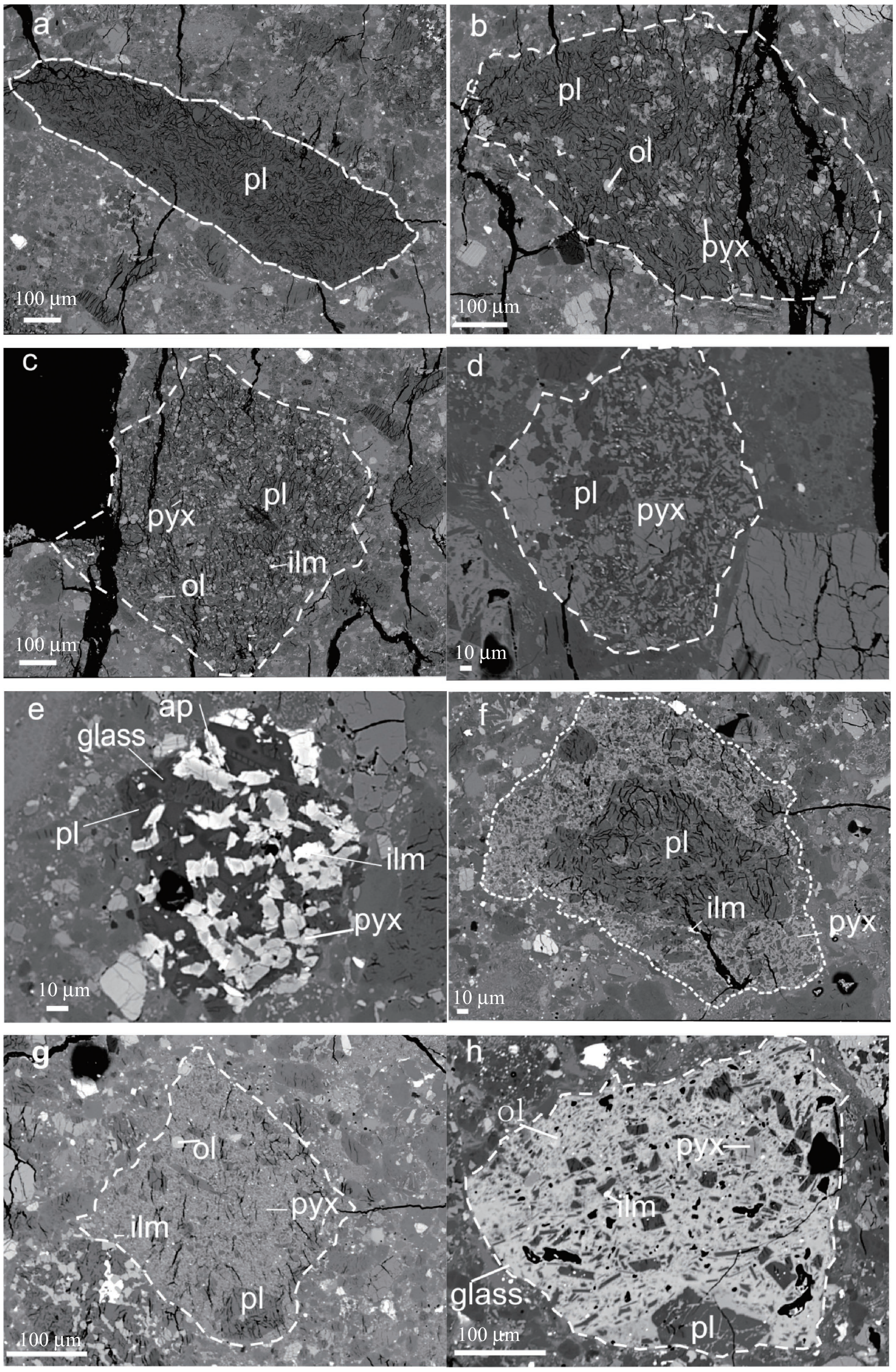

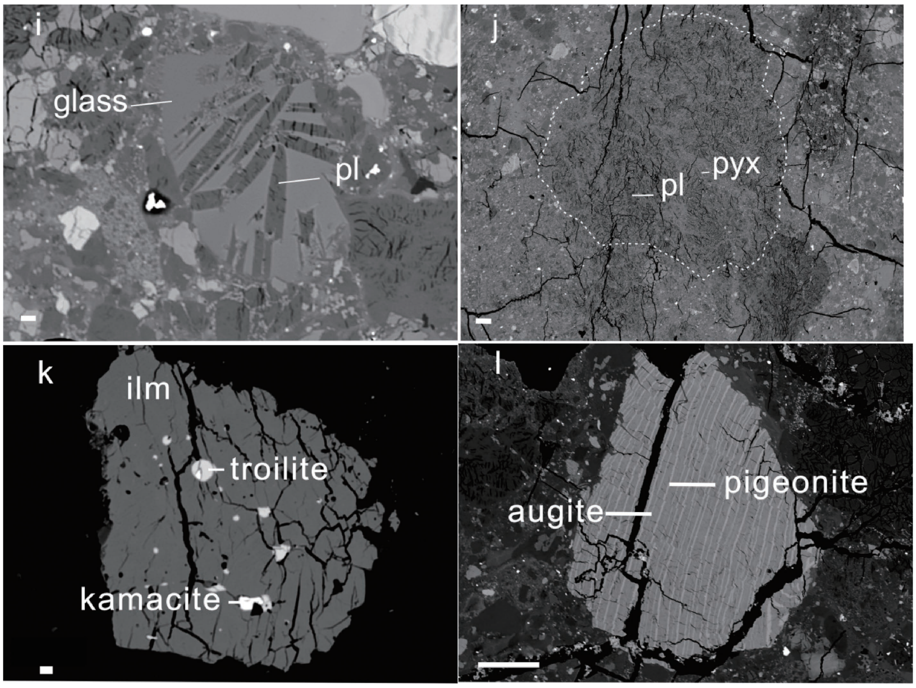

Figure 4 Backscattered electron images of the typical clasts in MIL090036, 26 (ap = apatite; pl = plagioclase; ilm = ilmenite; pyx = pyroxene; ol = olivine). Anorthosite clasts (**a**); Gabbroic anorthosite clasts (**b**); Troctolite clasts (**c**); Homeocrystalline gabbro clasts (**d**); Gabbro clasts with glass (**e**); Polymict clasts (**f**); Microporphyritic crystalline impact melt breccias (**g**); Glass melt breccias (**h**–**i**); Regolith clasts (**j**); Kamacite grain (**k**); Crystalloclastic pyroxene (**l**).

Table 1 The characteristics of various breccias in MIL090036, 26

Clast type	Number	Form	Structure	Mineral mode content and composition						
				Plagioclase		Pyroxene		Olivine		Other minerals
				vol.%	mineral	vol.%	mineral	vol.%	mineral	vol.%
Anorthosite	55	angular	massive broken	97-99	An_{88-95}	—	—	—	—	trace ilmenite
Gabbroic anorthosite	54	subrounded	granoblastic	77-82	An_{95-97}	16-30	$Fs_{19-26}Wo_{5-12}En_{57-62}$	1-5	Fa_{30-33}	ilmenite1-3
Troctolite	4	subangular	granoblastic	50-63	An_{91-93}	5-11	$Fs_{12-23}Wo_{8-40}En_{31-52}$	23-35	Fa_{26-28}	ilmenite, troilitr 1-3
Gabbro	5	subangular angular	equigranular porphyritic	50-55 29	An_{81-83} An_{95-98}	42-47 38	$Fs_{25-28}Wo_{7-13}En_{63-68}$ $Fs_{37-65}Wo_{5-35}En_{21-49}$	—	—	FeNi, troilite, ilmenite 1-3 glass 26, ilmenite 3, apatite 3
Polymict clast	2	angular	heterogranular	52-59	An_{95-98}	44-48	$Fs_{22-24}Wo_{5-35}En_{45-79}$	—	—	ilmenite 1-2
Regolith clast	21	subrounded	heterogranular	58-63	An_{93-97}	35-39	$Fs_{13-24}Wo_{3-36}En_{29-81}$	0-2	Fa_{24-30}	ilmenite 1-3
Microporphyritic crystalline impact melt breccia	22	angular	microphyric	30-37	An_{91-97}	55-62	$Fs_{19-23}Wo_{5-50}En_{19-54}$	0-3	Fa_{22-24}	ilmenite 1-3
Plagioclase	3	angular	monocrystal	100	An_{90-95}	—	—	—	—	—
Pyroxene	18	subangular	monocrystal	—	—	100	$Fs_{26-48}Wo_{2-33}En_{19-54}$	—	—	—
Olivine	2	angular	monocrystal	—	—	—	—	100	Fa_{21-31}	—
Ilmenite	2	subangular	monocrystal	—	—	—	—	—	—	ilmenite 98-100, FeNi, troilite 0-2
Feldsparthic glass clast	10	subrounded	porphyritic	25-65	An_{93-99}	0-14	$Fs_{12-27}Wo_{5-46}En_{29-72}$	0-3	Fa_{28-30}	glass 25-65, ilmenite, FeNi, troilite 0-3

anorthitic ($An_{81\text{-}98}$, avg. An_{92}) with 91% of An exceeding 90 mol% in all tested grains. Plagioclase with $An_{81\text{-}83}$ compositions are found in the homeocrystalline gabbro lithic clasts (Figure 4d) and plagioclase with average An_{90} are found in the anorthosite lithic clasts (Figure 4a). Plagioclase in other clasts have average compositions of $An_{>90}$ (Figure 5). The K_2O content of plagioclase is in the range of 0.11%–0.32% and Na_2O in the range of 0.11%–0.53%, except in the anorthosite lithic clast (1.10%) and gabbro lithic clast (2.14%). Representative analyses are presented in Table 2.

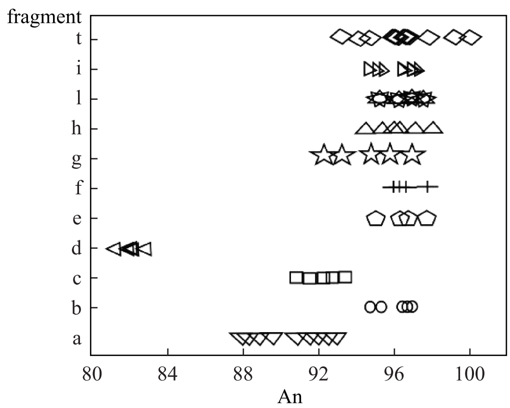

Figure 5 Anorthite (An) content in various clasts.

4.2 Olivine

The chemical composition data indicates that the olivine grains are mainly peridot and hyalosiderite in the forsterite–fayalite series. The compositional range of olivine ($Fo_{67\text{-}77}$) in the lithic clasts is narrower than that in the mineral grains and matrix ($Fo_{57\text{-}79}$)(Figure 6). The Fe and Mn content of olivine is mostly consistent with that of lunar material (Figure 7).

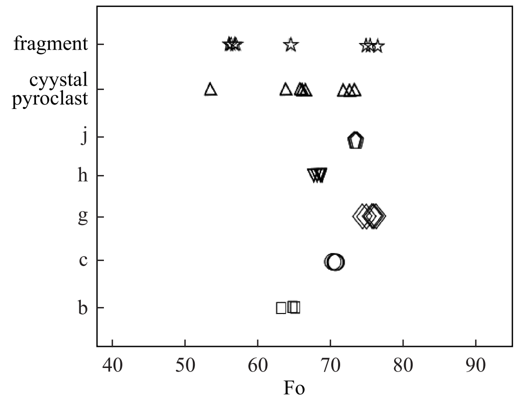

Figure 6 Forsterite (Fo) content in various clasts.

4.3 Pyroxene

There are a variety of pyroxene compositions evident in MIL090036, 26 (Figure 8). Pyroxene in lithic and glass clasts occurs predominantly as augite, pigeonite and minor calcium augite. Ferroaugite and calcium-deficient iron augite ($Fs_{37\text{-}65}$ $Wo_{10\text{-}29}$ $En_{21\text{-}49}$) were discovered only in gabbro clasts with glass (Figure 4e). Pigeonite is the sole pyroxene variety recognized in gabbroic anorthosite ($Fs_{19\text{-}26}$ $Wo_{5\text{-}12}$ $En_{57\text{-}62}$) (Figure 4b) with partially devitrified and homeocrystalline

Table 2 Representative analyses (wt.%) of the main minerals in various clasts in MIL090036, 26

	a	b			c			d		e			f		g		
	pl	ol	pyx	pl	ol	pl	pyx	pyx	pyx	pl	pyx	ilm	pl	pyx	pl	ol	pyx
Na_2O	1.10	0.02	0.10	0.41	0.04	1.01	0.36	2.52	0.03	2.14	0.12	bd	0.30	0.51	0.31	0.02	0.02
Al_2O_3	30.0	0.61	5.41	34.1	0.03	32.2	1.21	1.03	0.82	30.6	0.51	0.22	34.6	14.2	34.4	1.11	1.70
MgO	0.11	34.7	20.2	0.02	38.3	0.21	23.5	22.8	22.1	0.08	6.60	0.69	0.18	15.69	0.02	38.5	20.2
ZnO	bd	bd	bd	bd	bd	bd	bd	bd	bd	bd	bd	0.11	bd	bd	bd	bd	bd
K_2O	0.11	bd	bd	0.09	bd	0.28	0.02	0.40	bd	0.31	0.12	bd	bd	0.11	bd	bd	0.02
FeO	0.19	29.9	14.2	0.20	25.8	0.22	7.8	17.3	22.4	0.39	34.9	46.9	0.40	11.5	0.31	20.7	21.1
MnO	bd	0.59	0.28	0.21	0.31	bd	bd	0.02	0.62	0.10	0.50	0.59	bd	0.21	bd	0.21	0.62
Cr_2O_3	bd	bd	0.30	bd	0.14	bd	0.02	0.09	0.22	0.11	bd	0.21	bd	0.23	bd	0.02	0.54
PbO	bd	0.12	bd	0.02	bd	bd	bd	0.02	0.04	bd	bd	0.02	0.10	bd	bd	bd	bd
V_2O_3	bd	bd	0.02	0.13	bd	bd	bd	0.11	bd	0.10	0.04	0.10	bd	0.03	bd	bd	bd
CaO	20.6	0.02	6.50	20.7	0.21	19.7	20.5	6.4	2.22	20.2	7.20	0.41	20.9	10.8	20.5	0.70	5.33
NiO	bd	0.10	bd	bd	bd	bd	bd	bd	bd	bd	bd	bd	0.09	bd	bd	bd	bd
TiO_2	bd	bd	0.71	0.12	0.11	0.10	0.02	0.10	0.54	0.10	0.70	52.0	bd	1.80	bd	0.12	0.41
BaO	bd	0.11	bd	bd	bd	bd	0.10	bd	bd	bd	bd	bd	0.02	bd	0.11	0.02	bd
P_2O_5	bd	bd	bd	bd	bd	bd	bd	bd	bd	bd	bd	bd	bd	0.22	bd	bd	bd
SiO_2	46.3	33.4	52.8	43.8	33.3	46.5	47.9	50.4	52.4	45.3	49.7	0.62	44.7	44.7	42.9	38.9	50.7
Total	98.3	99.5	100.7	99.8	98.2	100.2	99.5	100.4	101.2	99.5	100.2	102.0	101.5	99.8	98.7	100.2	100.5
Fa/Fs/An	90	31	24	96	27	90	12	26	34	83	62		95	21	98	23	33
Fo/Wo/Ab	9	69	14	3	73	8	42	12	4	16	16		5	25	2	77	10

(Continued)

	g	h					i		j			min			mix		
	FeNi	ol	pl	pyx	FeNi	ilm	pl	glass	ol	pl	pyx	ol	pyx	pl	ol	pyx	Q
Na_2O	0.10	0.02	0.36	0.02	0.10	bd	0.28	0.49	0.02	0.51	0.30	0.02	0.02	0.30	bd	2.11	bd
Al_2O_3	1.41	0.11	18.4	2.60	1.40	2.11	36.5	25.7	0.08	36.8	9.11	bd	0.50	22.7	0.81	0.62	0.21
MgO	1.43	34.4	7.53	16.8	1.44	3.50	0.31	8.80	38.2	0.12	20.8	34.6	16.0	6.71	26.6	16.1	bd
ZnO	0.11	0.08	bd	bd	0.13	bd	bd	bd	0.04	bd	bd	bd	bd	bd	0.02	0.02	bd
K_2O	bd	bd	bd	bd	bd	0.01	bd	bd	0.11	bd	0.10	bd	bd	0.02	bd	0.28	bd
FeO	81.7	26.2	12.6	7.9	81.7	39.7	0.32	5.62	24.2	0.31	13.4	27.4	28.1	9.90	35.8	14.0	0.10
MnO	0.11	0.31	0.26	0.28	0.10	0.58	0.02	0.02	0.40	0.12	0.11	0.20	0.34	0.10	0.31	0.10	0.10
Cr_2O_3	0.10	0.40	0.31	0.82	0.10	0.54	bd	0.10	0.31	bd	0.49	0.10	0.10	0.23	bd	0.02	bd
PbO	0.09	bd	bd	0.07	0.08	0.21	bd	bd	bd	bd	bd	0.03	bd	bd	bd	bd	bd
V_2O_3	bd	0.10	bd	bd	bd	0.21	bd	bd	bd	bd	bd	bd	bd	bd	bd	bd	bd
CaO	1.51	0.62	14.4	21.0	1.52	2.84	20.2	15.1	0.54	20.3	7.52	0.18	2.30	14.9	0.22	14.7	0.10
NiO	7.44	bd	bd	bd	7.44	bd	bd	bd	bd	bd	bd	bd	bd	bd	bd	bd	bd
TiO_2	0.10	bd	0.59	1.88	0.10	42.8	0.11	0.60	0.02	0.10	1.74	bd	1.00	0.62	0.10	0.11	0.20
BaO	bd	bd	bd	0.09	bd	bd	bd	bd	bd	bd	0.02	bd	bd	bd	bd	bd	bd
P_2O_5	bd	bd	bd	bd	bd	0.02	bd	bd	bd	0.02	bd	bd	bd	bd	bd	bd	bd
SiO_2	3.62	38.4	45.2	45.4	3.61	6.62	43.6	44.1	39.0	43.6	45.4	36.7	50.3	45.4	35.0	53.5	97.4
Total	97.5	100.7	99.8	97.0	97.5	99.2	101.4	100.5	100.2	101.8	98.7	99.2	98.8	100.8	98.9	101.1	98.2
Fa/Fs/An		29	97.	12			98		26	97	22	30	47	98	29	22	
Fo/Wo/Ab		71	3	42			2		74	3	16	70	5	2	71	30	

Note: ol=olivine, pl=plagioclase, pyx=pyroxene, FeNi=FeNi metal, ilm=ilmenite, Q=quartz , min=mineral, mix=matrix, bd=below detectable limit.

gabbroic lithic clasts (Fs_{25-28} Wo_{7-13} En_{63-68}) (Figure 4d). Pyroxene in the feldspar glass (Figure 4h) occurs in a wide range of compositions, with augite, ferroaugite and pigeonite recognized. Similarly, pyroxene in microporphyritic impact melt breccias (Figure 4g), regolith breccia clasts (Figure 4j), and troctolite clasts (Figure 4c) has a wide range of compositions, from augite to calcium-deficient augite to pigeonite (components in order are: Fs_{19-23} Wo_{5-50} En_{31-62}, Fs_{13-24} Wo_{3-36} En_{29-81}, $Fs_{12-23}Wo_{8-40}$ En_{31-52}). Pyroxene in the matrix occurs predominantly as ferroaugite and pigeonite; relatively enriched in Fe compared to pyroxene in the lithic clasts (Figure 8). The Fe and Mn contents of the pyroxenes are mostly similar to lunar material (Figure 7).

4.4 Other minerals

All of the ferronickel in MIL090036, 26 is in the form of kamacite. Minor amounts of Al, Ti, Fe were found in quartz, as well as some chromite inclusions.

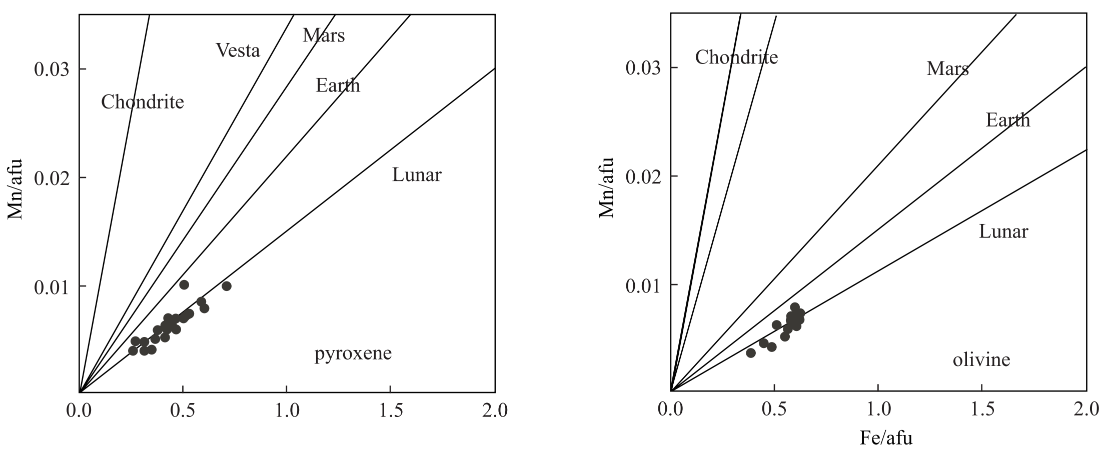

Figure 7 Fe and Mn contents of pyroxene and olivine in MIL090036, 26[9].

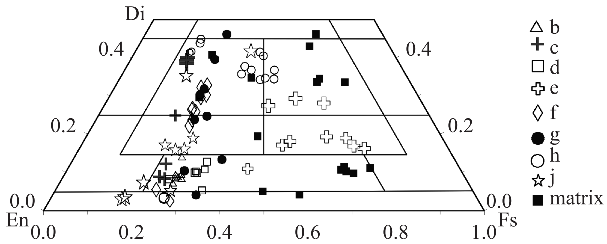

Figure 8 Quadrilateral diagram of pyroxene compositions occurring in MIL090036, 26: gabbroic anorthosite clasts (b); troctolite clasts (c); gabbro clasts (d); gabbro clasts with some glass (e); polymict clasts (f); microporphyritic crystalline impact melt breccia (g); glass melt breccia (h); regolith clasts (j).

4.5 Bulk composition

The bulk chemistry test results are presented in Table 3. The result is basically accordance with the previous results of other sections especially for the major elements, e.g. Fe, Mg, Al. And we calculated the ratios of Fe/Mn and (FeO+MgO)/Al_2O_3 are 83 and 0.4, respectively. Both of the plots in compositional fields associated with the lunar highlands of the Moon (Figures 9–10).

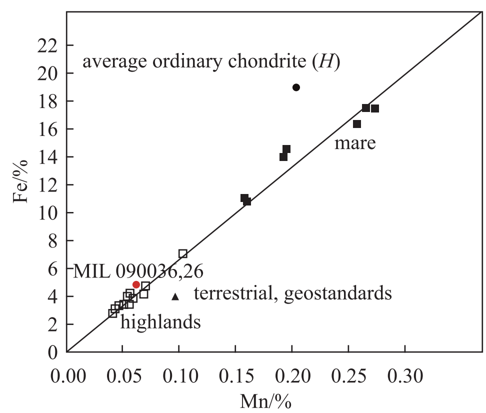

Figure 9 Bulk Fe/Mn compositional diagram for lunar meteorites[3].

5 Discussion

5.1 The lunar origin of MIL090036

There are four main lines of evidence that MIL09036 originated from the Moon:

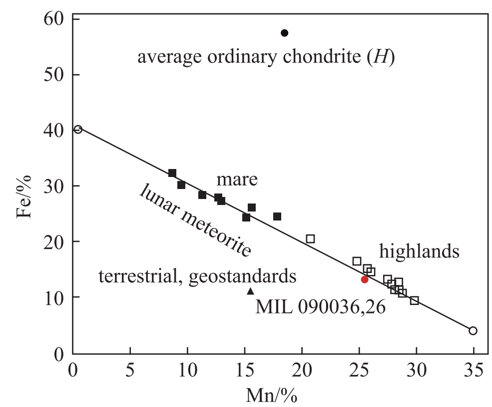

Figure 10 Bulk (FeO+MgO)/Al_2O_3 compositional diagram for lunar meteorites[3].

(1) The large number of varying clasts discovered in this specimen—the rock-forming minerals, including plagioclase, pyroxene, olivine and ilmenite are characteristic of other lunar breccias [3].

(2) The anorthite component of the plagioclase ($An_{90\text{-}98}$) is consistent with that found in other lunar meteorites ($An_{90\text{-}100}$), but is not consistent with plagioclase composition in howardite–eucrite–diogenite (HED) achondrites ($An_{80\text{-}100}$) [10].

(3) Mafic minerals in rock from the Earth, Moon, Mars, and asteroids have distinct Fe to Mn rations, our pyroxene and olivine chemistry data support a lunar origin for MIL090036.

(4) The bulk chemistry of Fe/Mn and (FeO+MgO)/(Al_2O_3) ratios also support the lunar highland origin for MIL090036, 26 (Figures 9–10).

5.2 Meteorite type

As discussed, MIL090036 is predominantly composed of various clasts, and has a fine-grained crystalline, glassy matrix. The clasts (>0.1 mm in size) are mainly lithic and feldspathic and predominantly fine- to very fine-grained. Both Fe/Mn and (FeO+MgO)/(Al_2O_3) ratios support a lunar highland origin for MIL090036.

The bulk chemistry of MIL090036, 26 (Al_2O_3 26.1%; FeO 5.01%) is comparable to lunar highland anorthosite (Al_2O_3 25–30 wt%; FeO 3–6 wt%)[11], indicating that MIL090036 is a lunar feldspathic breccia. According to Stöffler classification

Table 3 Bulk composition in MIL090036

	TiO_2	Al_2O_3	Cr_2O_3	FeO	MnO	MgO	CaO	Na_2O	K_2O	P_2O_5	SO_3	SiO_2
MIL090036,26	0.47	26.1	0.22	5.01	0.06	5.51	16.5	0.63	0.08	0.01	0.15	45.1
MIL090036,12[5]	—	28.3	—	3.02	<0.01	3.53	15.7	—	0.01	—	—	—
MIL090036,13[5]	—	27.2	—	4.12	<0.01	4.33	14.8	—	0.01	—	—	—
MIL090036[7]	0.59	27.4	—	—	—	4.82	—	0.68	—	—	—	—
MIL090036[6]	—	—	—	3.75—5.54	—	—	—	0.55—0.72	—	—	—	—
MIL090036[8]	—	26.3	—	—	—	—	—	—	—	—	—	—

criteria[12], such as texture, structure, grain-size and petrography and chemistry of matrix and clasts, MIL090036 can be further classified as a plagioclase polymict breccia.

5.3 Provenance determination of MIL090036

MIL090034, MIL090070 and MIL090075, also feldspathic breccias, were collected in the Miller Range of Antarctica at the same time as MIL090036. Petrographic and geochemical studies have shown that MIL090034, MIL090070 and MIL090075 came from the same meteorite[7]. Compared with MIL090036 the former three meteorites have lower FeO and Na_2O contents and higher Al_2O_3 content. All four meteorites are clast-rich, feldspathic breccias. However MIL090034, MIL090070, MIL090075 mainly contain weathered breccia clasts, with very low anothosite, gabbroic anorthosite and clast content compared with MIL090036. A concentration of 1.7 ppm of Th was determined in MIL090036, compared with 0.3 ppm, 0.3 ppm and 1.1 ppm in MIL090034, MIL090070 and MIL090075, respectively[6]. While MIL090034, MIL090070 and MIL090075 have negative Eu anomalies it can be noted that MIL090036 has a positive Eu anomaly, comparable to feldspathic lunar meteorite NWA4936 and samples from Apollo 16[8]. The chemical-petrographic type of MIL090036 shares certain characteristics with the samples of Apollo16, such as the feldspathic breccia character that basically consistent with 50 samples from Apollo16 mission[13]. However, MIL090036 is more deficient in aluminum (Figure 11) and has a different modal abundance of pyroxene and feldspar to samples collected by both the Apollo 16 and Luna missions (Table 4).

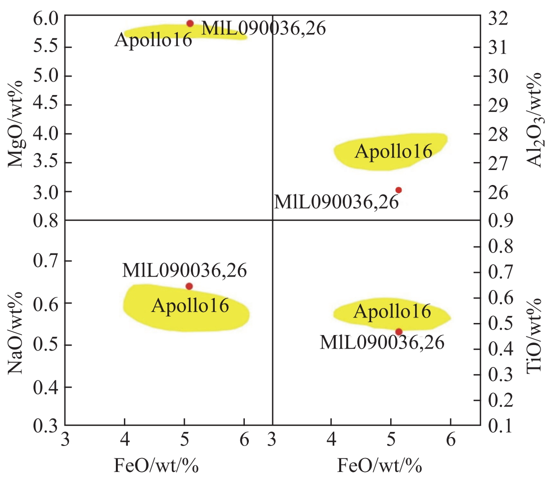

Figure 11 Major element composition of MIL090036, 26 in comparison to Apollo16 samples[7].

Table 4 Modal mineralogy of MIL090036, 26

	plagioclase	olivine	pyroxene	quartz	opaque mineral
MIL090036	63	2.8	34	0.1	0.3
Apollo16[14]	69	2.6	28.2	—	0.1

It is evident from the above that, although MIL090036 is a clearly a lunar meteorite, it originates from an area outside of that sampled by both the Apollo and Luna missions.

5.4 The significance of lunar meteorite MIL090036

MIL090036 is a plagioclase polymict lunar breccia consisting of fine-grained material originating from near the lunar surface. After strong impact, consequent breccia formation and mixing, this lunar breccia can be considered to be more representative of the average geochemical and mineralogical composition of the Moon than other unbrecciated rock from the same area[3]. It is also in itself a record of the early meteorite impacts of the Moon[15].

Given that MIL090036 likely originated from an area outside of that sampled by the Apollo and Luna missions, it will provide significant supplementary opportunity for research of the lunar crust, particularly in terms of understanding the spatial distribution of rock types within the lunar crust.

According to previous reports, MIL090036 contains higher concentrations of incompatible elements than other feldspathic lunar meteorites; the 1.7 ppm Th content indicates a possible KREEP component in clasts of this meteorite[6] (KREEP = potassium, rare earth elements, phosphorous). Given that the meteorite is a breccia mixture, of a variety of source materials, no KREEP clasts were found in this study; however, their existence cannot be precluded. If the KREEP component can be proved, it would not only provide an indication of the distance between meteorite source area and the Imbrium Basin center[16], but may also provide evidence for an abundant extra-terrestrial rare earth element resource.

Acknowledgements This study was supported by the Natural Science Foundation of China (Grant no. 41173077) and the Director Fund of Guangxi Key Laboratory of Hidden Metallic Ore Deposits Exploration (Grant no. 13-A-01-02). Sample was provided by National Aeronautics and Space Administration (NASA)Johnson Space Center. Resource-sharing Platform of Polar Samples (http://birds.chinare.org.cn)maintained by Polar Research Institute of China(PRIC) and Chinese National Arctic & Antarctic Data Center(CN-NADC) offers help in the process of this thesis writing.

References

1 Korotev R L. Lunar geochemistry as told by lunar meteorite. Chemie der Erde-Geochemistry, 2005, 65(4): 297-346.

2 Warren P H. A concise compilation of petrologic information on possibly pristine nonmare Moon rocks. American Mineralogist, 1993, 78: 360-376.

3 Ou Yang Z Y. Introduction to lunar science. Beijing: China Astronautic Publishing House, 2005 (in Chinese).

4 Wang D D. New developments in the study of meteorite. Chinese Journal of Nuture, 1995, 17 (1): 13-17 (in Chinese).

5 Korotev R L, Joliff B L, Carpenter P K. Miller range feldsparthic lunar meteorite // Proceedings of the 42nd Lunar and Planetary

Science Conference. The woodlands: LPI, 2011: 1999.
6 Zeigler R A, Korotev R L, Jolliff B L. Pairing relationships among feldspathic lunar meteorites from Miller Range, Antarctica // Proceedings of the 43rd Lunar and Planetary Science Conference. The Woodlands: LPI, 2012: 2377.
7 Nishizumi K, Caffee M W. Relationship among six meteorites from MillerRange, Antarctica based on cosmogenic radionuclides // Proceedings of the 44th Lunar and Planetary Science Conference, 2013: 2715.
8 Shirai N, Ebihara M, Sekimoto S, et al. Geochemistry of lunar highland meteorites MIL090034, 090036 and 090070 // Proceedings of the 43rd Lunar and Planetary Science Conference. The Woodlands: LPI, 2012: 2003.
9 Papike J J. Comparative planetary mineralogy: Chemistry of melt-derived pyroxene, feldspar, and olivine // Proceedings of the 29th Annual Lunar and Planetary Science Conference. Houston: LPI, 1998: 1008.
10 Wang D D, Lin Y T. Ispiration from study of antarctic meteorite Ⅲ: Overview on antarctic lunar meteorite and their evolutional history. Chin J Polar Res, 1993, 5(2): 1-20 (in Chinese).
11 Hsu W B, Zhang A C, Bartoschewitz R, et al. Petrography, mineralogy, and geochemistry of lunar meteorite Sayh al Uhaymir 300. Meteoritics & Planetary Science, 2008, 43(8): 1363-1381.
12 Stoffler D, Knoell H D, Marvin U B, et al. Recommended classification and nomenclature of lunar highland rocks-a committee report // Proceedings of the Conference on the Lunar Highlands Crust. New York and Oxford: Pergamon Press, 1980: 51-70.
13 Chao E C T. Preliminary genetic classification of Apollo 16 breccias. Lunar and Planetary Science Conference, 1973, 4: 129.
14 Basu A, Riegsecker S E. Reliability of calculating average soil composition of apollo landing sites. Workshop on New Views of the Moon: Integrated Remotely Sensed, Geophysical, and Sample Datasets, 1998: 20.
15 Zhang A C, Hsu W B. Petrographic and mineralogical studies of the lunar meteorite Dhofar 1180. Aca Petrologica Sinica, 2007, 23(5): 1160-1168 (in Chinese).
16 Zhang A C, Hsu W B. A KREEP clast in the lunar meteorite Dhofar 1180. Lunar and Planetary Science, 2007, XXXVIII: 1108.